Submitted to
31st International Conference on High Energy Physics, ICHEP02, July 24, 2002, Amsterdam
Abstract: **991**
Parallel Session **6**
www-h1.desy.de/h1/www/publications/conf/conf_list.html

Photoproduction of ρ Mesons with a Leading Proton at H1

H1 Collaboration

Abstract

The elastic photoproduction of rho mesons is studied with the H1 detector in events where a high momentum proton is measured in the forward proton spectrometer. The photon-proton centre-of-mass energy is in the range $25\ \mathrm{GeV} < W < 70\ \mathrm{GeV}$, the four momentum transfer squared at the proton vertex is $0.073\ \mathrm{GeV}^2 < |t| < 0.45\ \mathrm{GeV}^2$ and the fractional energy of the proton is $E_{p'}/E_p > 0.98$. The distribution of the two pion invariant mass is found to be skewed increasing with decreasing $|t|$. A variation with W is not observed. The total cross section for rho meson photoproduction is measured in three bins of W, as well as the slope of the differential cross section $\mathrm{d}\sigma/\mathrm{d}t \propto \exp(bt)$. The measured slope $\alpha'_{\mathbb{P}}$ of the pomeron trajectory is compatible with a gradient $\alpha'_{\mathbb{P}} = 0.25\ \mathrm{GeV}^{-2}$ extracted from fits to hadron-hadron elastic scattering cross sections. The results of an analysis of the decay angular distribution are compatible with the assumption of s-channel helicity conservation in this process.

1 Introduction

The observation of exclusive ρ vector meson production in γp interactions is a manifestation of the hadronic content of the photon. The reaction is described by assuming that the photon fluctuates into a ρ meson according to the vector meson dominance model (VDM), which scatters off the proton so that the process resembles in all features a hadronic interaction. The interpretation of the photoproduction process in terms of an elastic scattering of ρ mesons on a proton makes it possible to treat this process as a diffractive process, which is at high energies dominated by a pomeron exchange. In addition to the hadronic aspects of the reaction, further photoproduction properties can be accessed via a study of the ρ line shape and the ρ polarisation.

The analysis presented here is based on data collected between January and April 1999, when HERA collided 920 GeV protons with 27.5 GeV electrons, corresponding to an ep centre-of-mass energy of $\sqrt{s} = 320$ GeV.

2 The Forward Proton Spectrometer (FPS)

The FPS [2] is used to measure the four momentum of the scattered proton. It consists of fibre hodoscopes, sandwiched between trigger scintillators, installed in movable "Roman Pot" plunger vessels. Two identical stations are installed at 64 m and 80 m from the interaction point[1]. Together with the magnets of the HERA beamline it forms a magnetic spectrometer. Scattered protons with a different energy and/or angle compared to the nominal beam protons will be separated from the circulating beam and can be detected at appropriate positions.

The error on the energy measurement amounts to about 5.5 GeV, which is 0.6% of the beam energy. The position of the detectors with respect to the nominal interaction point, together with their distance from the beam and the beamline aperture, restrict the FPS acceptance to proton transverse momenta squared $-t \approx p^2_{t,p'}$ of $0.073\ \text{GeV}^2 < p^2_{t,p'} < 0.45\ \text{GeV}^2$ and proton energies of $E_{p'} > 900$ GeV.

3 Data Selection and Correction

The FPS detectors were in a stable position close to the circulating beam and all relevant components of the H1 detector were required to be fully operational. Events were triggered by demanding a proton candidate in the FPS, at least one track candidate in the central jet chamber and a reconstructed vertex. The corresponding integrated luminosity was 3 pb^{-1}. Events were selected in which

- the four momentum of the scattered proton could be reconstructed in the FPS,

[1] At 81 m and 90 m two more detectors are installed. For acceptance reasons these are not used in the analysis presented here.

- exactly two unlike-sign tracks in the central jet chamber could be reconstructed and no further tracks in the forward tracking chambers were found,
- the specific ionization $\mathrm{d}E/\mathrm{d}x$ of the two tracks was consistent with a pion hypothesis and
- no electron was identified in the H1 calorimeter.

In addition, the following selection criteria were applied to ensure a sufficiently high acceptance and efficiency:

- The transverse momentum of the higher energetic pion is restricted to $p_t > 0.45$ GeV.
- The photon-proton centre-of-mass energy is limited to 25 GeV$< W < 70$ GeV.
- The invariant two pion mass is in the range of 0.6 GeV $< M_{\pi\pi} < 1.1$ GeV.
- The energy fraction kept by the scattered proton is restricted to $z = E_{p'}/E_p > 0.98$.

The virtuality Q^2 of the incident photon is restricted to $Q^2 < 1$ GeV^2 by demanding that the scattered electron is not detected in the H1 detector. The average Q^2 of the data estimated with a Monte Carlo simulation is found to be $\langle Q^2 \rangle \approx 10^{-4}$ GeV^2.

The data are corrected for the efficiencies and acceptances of the detector components using a Monte Carlo simulation. The total probability for reconstructing a proton in the FPS for this reaction is 20%. The probability for reconstructing two tracks in the H1 central detector varies from about 5% for $M_{\pi\pi} = 0.6$ GeV to 20% for $M_{\pi\pi} = 1.1$ GeV. These values include the geometrical acceptance and the trigger and reconstruction efficiencies.

4 Background and systematic errors

The following sources of background are studied:

- Proton dissociation: If the proton dissociates into a multi-particle system only the most energetic of these particles reach the FPS detectors. Simulation studies show that the acceptance for protons for $z = E_{p'}/E_p > 0.98$ is zero, so that no background contamination from proton dissociative processes is present in the selected data.
- Beam induced background: Proton diffractive interactions with the residual gas can lead to events where the scattered beam proton is observed in the FPS and two tracks are reconstructed in the central detector. Typically one of these tracks is a proton and is rejected by the $\mathrm{d}E_\pi/\mathrm{d}x$ requirement. The remaining background contribution is determined to be 1% and is included as a systematic error. The contribution of protons arising from random overlap events in the FPS has been measured to be less than 0.075% and is neglected.
- ϕ and ω vector mesons: Decays of the ϕ and ω mesons into K^+K^- and $\pi^+\pi^-\pi^0$ respectively could fake a ρ meson. Simulation studies show that, in the mass and energy range considered, the contributions from these processes are negligible.

The systematic errors are grouped into those originating from the measurement of the ρ meson in the central detector and those originating from the measurement of the proton in the FPS. The former amounts to 8.3% and the latter ranges between 7.5% and 10.6%, depending on $|t|$. The total error is therefore 11% to 13%. The different contributions are listed in Table 1.

5 Results

The differential cross section $\mathrm{d}\sigma/\mathrm{d}M_{\pi\pi}$ for $25\ \mathrm{GeV} < W < 70\ \mathrm{GeV}$ and $0.073\ \mathrm{GeV}^2 < |t| < 0.45\ \mathrm{GeV}^2$ is shown in Figure 1. The $\pi^+\pi^-$ invariant mass distribution is found to be skewed. In the Söding Model [5] this is attributed to an interference between resonant (described by a Breit-Wigner resonant curve) and non-resonant production of $\pi^+\pi^-$ pairs. The differential cross section $\mathrm{d}\sigma/\mathrm{d}M_{\pi\pi}$ for the two pions can be expressed as

$$\frac{\mathrm{d}\sigma}{\mathrm{d}M_{\pi\pi}} = f_\rho BW_\rho(M_{\pi\pi}) + f_I I(M_{\pi\pi}) + f_{\mathrm{NR}} \tag{1}$$

where $f_\rho BW_\rho(M_{\pi\pi})$ describes the resonant, $f_I I(M_{\pi\pi})$ the interference and f_{NR} the constant non-resonant background contribution. f_ρ and f_I are normalisation parameters. The data are fitted to the Söding Model in Figure 1.

In the Ross-Stodolsky Model [6] the two pion mass spectrum is accounted for using a mass dependent production amplitude. The skewing parameter n is found to increase with decreasing $|t|$, a variation with W is not observed (Figure 2). The $|t|$-dependence is in agreement with the measurement of the ZEUS collaboration [7].

The cross section for resonant ρ meson production, measured for the accessible $|t|$ and W range and extrapolated to the range $2M_\pi < M_{\pi\pi} < M_\rho + 5\Gamma_\rho$ (i.e. $0.28\ \mathrm{GeV} < M_{\pi\pi} < 1.52\ \mathrm{GeV}$), is $\sigma = (4.61 \pm 0.42(stat.) \pm 0.55(\mathrm{syst.}))\ \mu$b. It is determined by integrating the resonant part $f_\rho BW_\rho(M_{\pi\pi})$ in Equation 1 over the mass range considered.

The $|t|$ spectrum is measured directly with the forward proton spectrometer. The differential cross section $\mathrm{d}\sigma/d|t|$ is shown in five bins of $|t|$, corrected for acceptances and efficiencies, in Figure 3. A fit to $\mathrm{d}\sigma/d|t| = A_\rho\ \exp(-b_\rho|t|)$ yields the slope parameter $b_\rho = (10.31 \pm 0.77(\mathrm{stat.}) \pm 0.52(\mathrm{syst.}))\ \mathrm{GeV}^{-2}$ (for $\langle W \rangle = 38.1$ GeV). As a cross check a fit to the $M_{\pi\pi}$ spectrum was made in 3 $|t|$-bins and the differential cross section $\mathrm{d}\sigma/d|t|$ was calculated by integrating $f_\rho BW_\rho(M_{\pi\pi})$ in Equation 1. The resulting resonant cross sections are also plotted in Figure 3 and are in agreement with the first method.

The slope of the pomeron trajectory is determined by measuring b_ρ in three different W intervals corresponding to central values of $\langle W \rangle = 29.5, 40.9$ and 57.0 GeV. The values of b_ρ are plotted as a function of W in Figure 4. A fit of the form $b_\rho(W) = b_0 + 2\alpha'_{\mathbb{P}} \ln(W^2)$ leads to an extracted slope of the pomeron trajectory of $\alpha'_{\mathbb{P}} = 0.3 \pm 0.4\ (\mathrm{stat.})\ \mathrm{GeV}^{-2}$. Results for b_ρ from fixed target and HERA experiments are shown for comparison.

An extrapolation of the cross section $\sigma(ep \to e'\rho p')$ to the ranges $2M_\pi < M_{\pi\pi} < M_\rho + 5\Gamma_\rho$ and $|t|_{\min} < |t| < 0.5\ \mathrm{GeV}^2$ is performed with the measured b_ρ-values and leads to the result $\sigma(\gamma p \to \rho p) = (9.59 \pm 0.80(\mathrm{stat.}) \pm 1.15(\mathrm{syst.}))\ \mu\mathrm{b}$ (for $\langle W \rangle = 38.1$ GeV). The values for

the different W-bins are plotted in Figure 5. In addition results from other experiments and a fit performed by Donnachie and Landshoff [9] are shown. The W dependence of the cross section is found to be compatible with a behaviour W^{δ} where $\delta = 4(1.08 - \alpha'/b_{\rho} - 1) \approx 0.22$ as expected for pomeron exchange in this centre-of-mass energy range.

By analysing the decay angular distribution of the two pions, two elements of the spin density matrix can be extracted (r^{04}_{00}, the probability of longitudinally produced ρ mesons, and r^{04}_{1-1}, the probability of a helicity double flip). These are measured to be $r^{04}_{00} = 0.030 \pm 0.030(\mathrm{stat.}) \pm 0.010(\mathrm{syst.})$ and $r^{04}_{1-1} = -0.017 \pm 0.032(\mathrm{stat.}) \pm 0.020(\mathrm{syst.})$.

6 Conclusions

The elastic photoproduction of ρ mesons has been studied using the H1 detector by measuring the final state proton with a forward proton spectrometer. The measurement extends the centre-of-mass energy range to $25\ \mathrm{GeV} < W < 70\ \mathrm{GeV}$, thereby further reducing the kinematic separation between HERA and fixed-target measurements. The data are free from contributions where the proton is excited into a lower mass state. The total background level is in the order of 1%. The analysis is based on an integrated luminosity of $3\ \mathrm{pb}^{-1}$.

The results presented are, within errors, in agreement with assumptions of the vector meson dominance model and Regge theory: The result of the decay angular distribution analysis shows a compatibility with the assumption that s-channel helicity is conserved in this process. The measured slope of the pomeron trajectory is compatible with a value of $\alpha'_{\mathbb{P}} = 0.25\ \mathrm{GeV}^2$ from other experiments [8]. Both $b_{\rho} = (10.31 \pm 0.77(\mathrm{stat.}) \pm 0.52(\mathrm{syst.}))\ \mathrm{GeV}^{-2}$ and $\sigma(\gamma p \to \rho p) = (9.59 \pm 0.80(\mathrm{stat.}) \pm 1.15(\mathrm{syst.}))\ \mu\mathrm{b}$ are in a good agreement with earlier results from H1 and ZEUS. In addition, the W dependence of the total cross section is in agreement with a parameterisation from Donnachie and Landshoff [9].

References

[1] H1 Collaboration, I. Abt *et al.* Nucl. Instrum. Meth. A **386** (1997) 310.

[2] P. Van Esch *et al.*, Nucl. Instrum. Meth. A **446** (2000) 409.

[3] J. J. Sakurai, Phys. Rev. Lett. **22** (1969) 981.

[4] K. Goulianos, Phys. Rep. **101** (1983) 169.

[5] P. Söding, Phys. Lett. **19** (1966) 702.

[6] M. Ross and L. Stodolsky, Phys. Rev. **149** (1966) 1172.

[7] ZEUS-Collaboration, M. Derrick *et al.*, Eur. Phys. J. **C 2** (1998) 247.

[8] A. Donnachie and P. V. Landshoff, Nucl. Phys. **B 231** (1984) 189.

[9] A. Donnachie and P. V. Landshoff, Phys. Lett. **B 296** (1992) 227.

Error source		
Luminosity measurement	1.3%	
Trigger efficiency	7 %	
Track reconstruction efficiency in the central tracking chamber	3 %	
Pion identification	3 %	
Background	1 %	
Sum: ρ meson measured in H1		8.3%
Track reconstruction efficiency of protons in the FPS	4 %	
Momentum reconstruction efficiency of protons in the FPS	4 %	
FPS acceptance ($\|t\|$-dependent)	5 . . . 9%	
Sum: proton measured in the FPS		7.5 . . . 10.6%
Total Sum		11 . . . 13 %

Table 1: The sources of systematic errors.

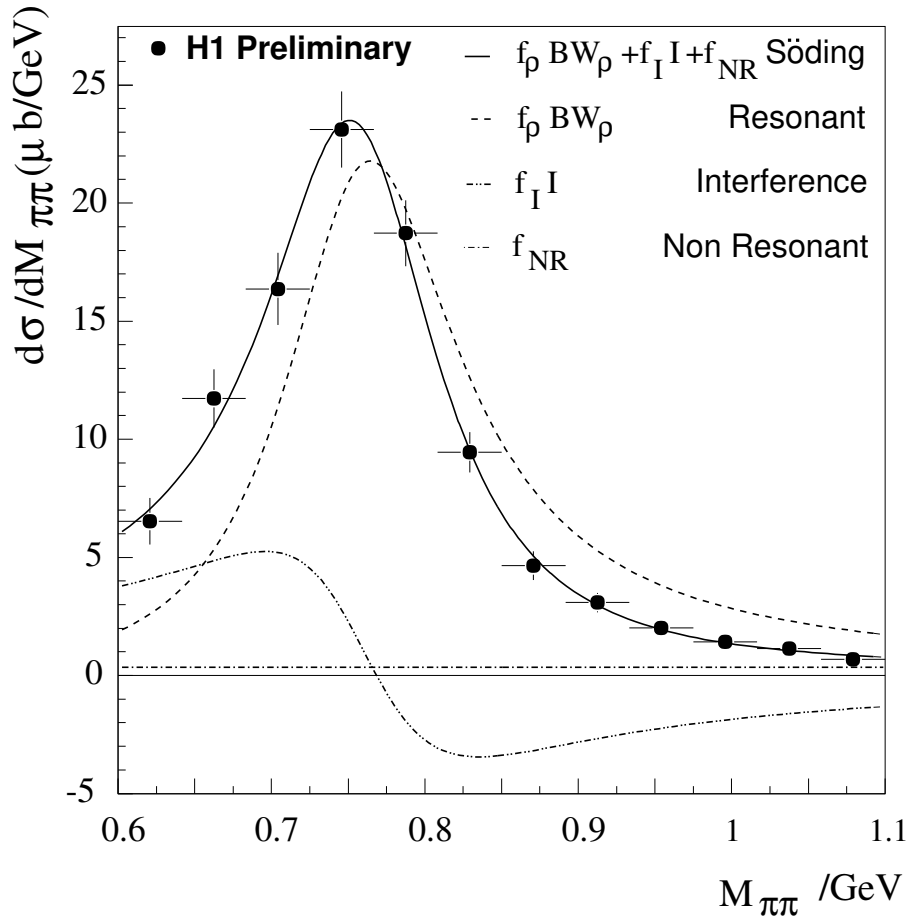

Figure 1: The spectrum of the two pion invariant mass. The different contributions of the Söding-Model are plotted.

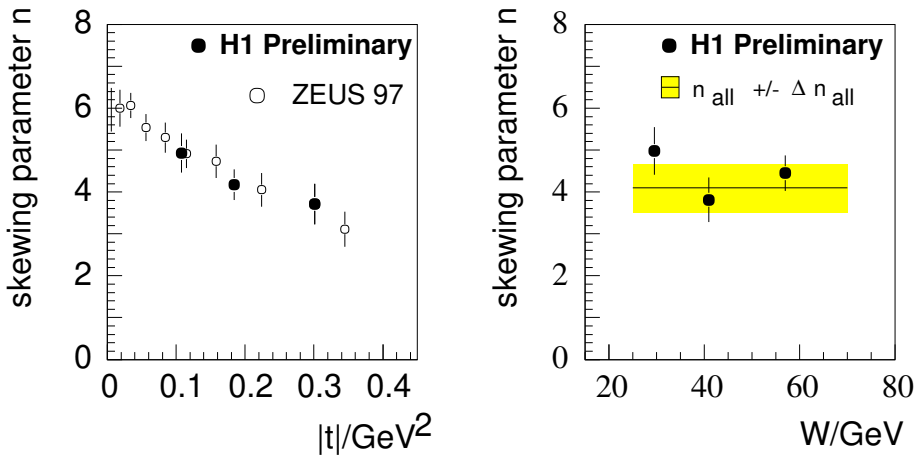

Figure 2: The $|t|$- and W-dependence of the skewing parameter n of the Ross-Stodolsky fit. Statistical errors are shown only. In the right plot in addition the skewing parameter n_{all} for the whole W-range and its error Δn_{all} is plotted.

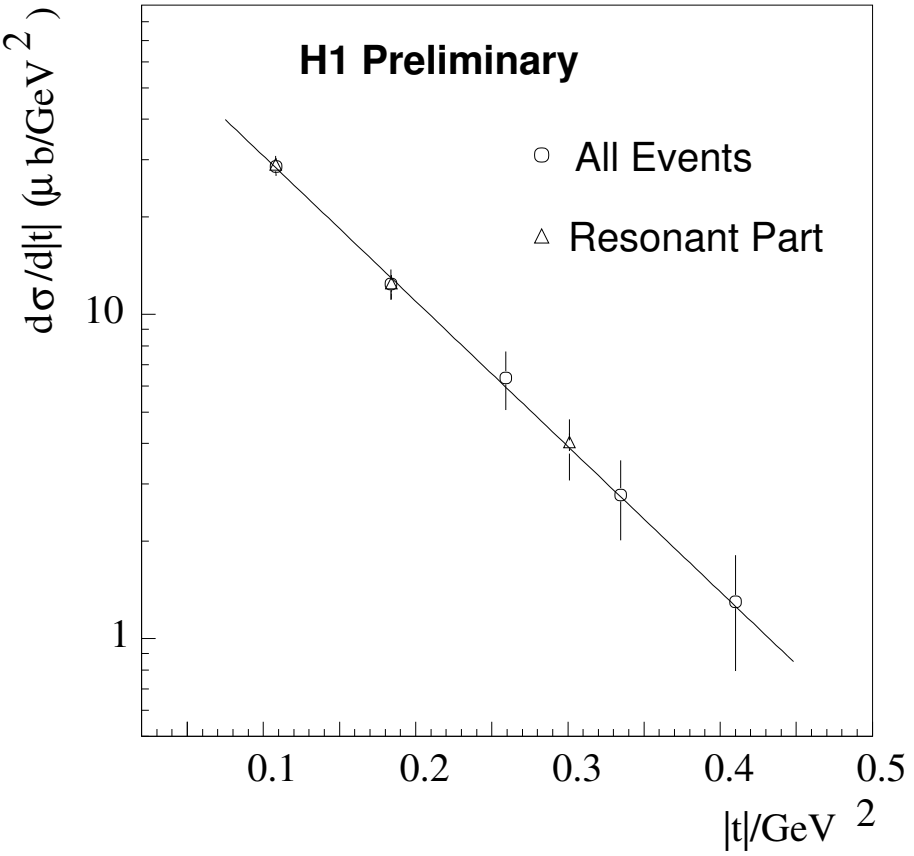

Figure 3: The differential cross section $\mathrm{d}\sigma/\mathrm{d}|t|$ measured with the FPS and fitted with a function $\mathrm{d}\sigma/\mathrm{d}|t| = A_\rho \exp\left(b_\rho|t|\right)$. The triangles represent $\mathrm{d}\sigma/\mathrm{d}|t|$ determined by integrating over the Breit-Wigner distribution from Equation 1 in 3 different $|t|$-bins. The error bars show the squared sum of the statistical and systematical error.

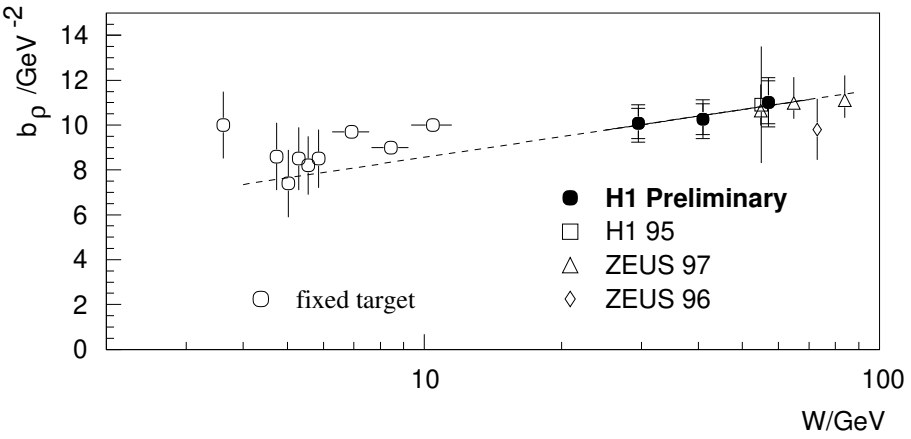

Figure 4: The values for b_ρ for the different W-bins, which are fitted with $b_\rho(W) = b_0 + 2\alpha'_{\mathbb{P}} \ln(W^2)$. The inner error bars represent the statistical errors and the outer ones the squared sum of the statistical and systematical error.

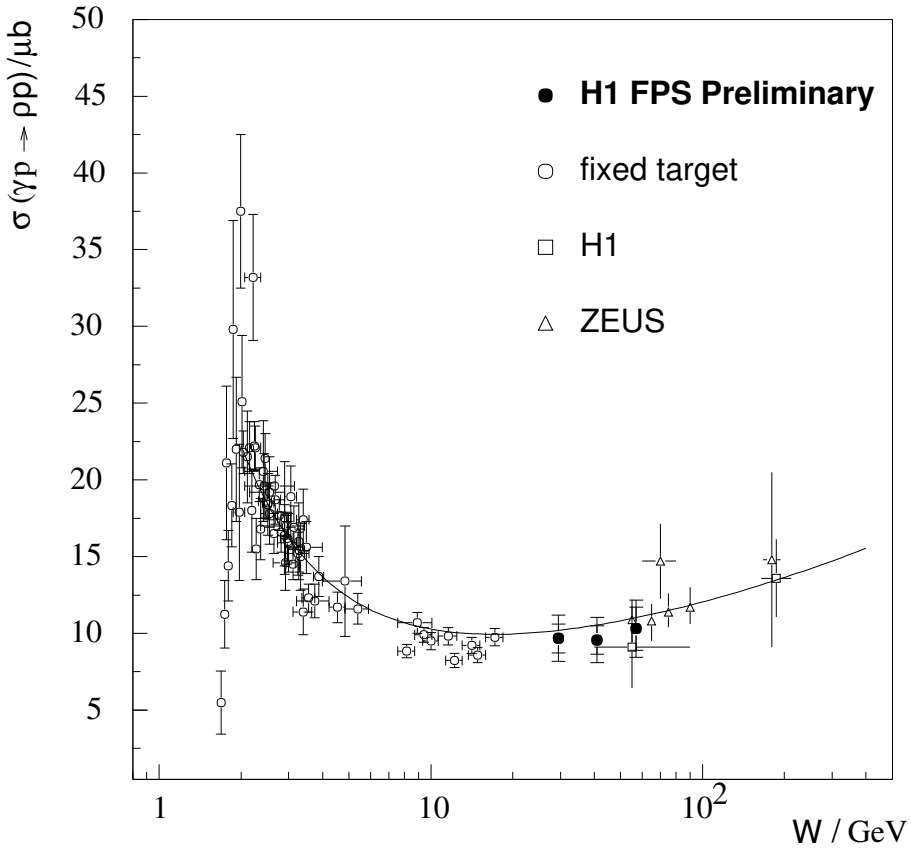

Figure 5: The ρ meson production cross section $\sigma(\gamma p \to \rho p')$ of this analysis for three W-bins and $|t| < 0.5$ GeV compared to other measurements and a fit of Donnachie and Landshoff. The inner error bars represent the statistical errors and the outer ones the squared sum of the statistical and systematical error.